ACS APPLIED MATERIALS & INTERFACES

Forum Article

www.acsami.org

Chemical and Structural Indicators for Large Redox Potentials in Fe-Based Positive Electrode Materials

Brent C. Melot,[†,‡] David O. Scanlon,[§,⊥] Marine Reynaud,[†] Gwenaëlle Rousse,[#] Jean-Noël Chotard,[†] Marc Henry,[∥] and Jean-Marie Tarascon*[,○]

[†]Laboratoire de Réactivité et Chimie des Solides, Université de Picardie Jules Verne, CNRS UMR 7314, 33 rue Saint Leu, 80039 Amiens, France

[‡]Department of Chemistry, University of Southern California, Los Angeles, California 90089, United States

[§]Kathleen Lonsdale Materials Chemistry Department of Chemistry, University College London, 20 Gordon Street, London WC1H 0AJ, United Kingdom

[⊥]Diamond Light Source Ltd., Diamond House, Harwell Science and Innovation Campus, Didcot, Oxfordshire, OX11 0DE, United Kingdom

[#]Institut de Minéralogie et de Physique des Milieux Condensés, Université Pierre et Marie Curie UPMC Univ Paris 06, CNRS UMR 7590, 4 Place Jussieu, 75252 Paris Cedex 05, France

[∥]Tectonique Moléculaire du Solide, UMR CNRS 7140, Université Louis Pasteur, Institut Le Bel, 4 Rue Blaise Pascal, 67070 Strasbourg Cedex, France

[○]College de France, 11 Place Marcelin Berthelot, 75000 Paris, France

ABSTRACT: Li-ion batteries have enabled a revolution in the way portable consumer-electronics are powered and will play an important role as large-scale electrochemical storage applications like electric vehicles and grid-storage are developed. The ability to identify and design promising new positive insertion electrodes will be vital in continuing to push Li-ion technology to its fullest potential. Utilizing a combination of computational tools and structural analysis, we report new indicators which will facilitate the recognition of phases with the desired redox potential. Most importantly of these, we find there is a strong correlation between the presence of Li ions sitting in close-proximity to the redox center of polyanionic phases and the open circuit voltage in Fe-based cathodes. This common structural feature suggests that the bonding associated with Li may have a secondary inductive effect which increases the ionic character of Fe bonds beyond what is typically expected based purely on arguments of electronegativity associated with the polyanionic group. This correlation is supported by ab initio calculations which show the Bader charge increases (reflecting an increased ionicity) in a nearly linear fashion with the experimental cell potentials. These features are demonstrated to be consistent across a wide variety of compositions and structures and should help to facilitate the design of new, high-potential, and environmentally sustainable insertion electrodes.

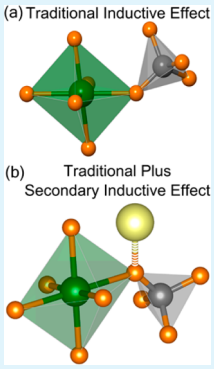

KEYWORDS: *inductive effect, ionicity, batteries, Lithium*

INTRODUCTION

Since their commercialization by Sony[1] more than two decades ago, Li-ion batteries have dominated the market as a tool for portable energy storage, and now there is significant interest in developing Li-ion batteries for use in larger volume applications such as electric transportation or stationary storage. Such large-scale applications, however, have far more challenging requirements compared to portable devices in terms of energy density, safety, cost, and sustainability.[2,3] Significant effort has, therefore, been devoted to searching for new materials that can be produced from abundant and low-cost resources. Given that iron is the most abundant transition metal in the Earth's crust, this would clearly be the most logical choice for a redox center; however, Fe-based cathodes are not ideal because the Fe^{3+}/Fe^{2+} redox-couple tends to operate at relatively low potentials compared to elements like Co or Mn.

Over the years, several strategies have been developed to raise the potential of these Fe-based phases. John Goodenough first showed that increasing the electronegativity of the anionic groups, which thereby increases the ionic character of the transition metal bonds, in the isostructural NASICON frameworks resulted in an increased open circuit voltage by as much as 0.8 V.[4,5] This argument, based purely around electronegativity, proved extremely robust and, indeed, can explain many of the trends observed for a variety of polyanionic groups such as those illustrated in Figure 1. Following similar

Special Issue: New Materials and Approaches for Electrochemical Storage

Received: December 4, 2013
Accepted: February 18, 2014
Published: March 3, 2014

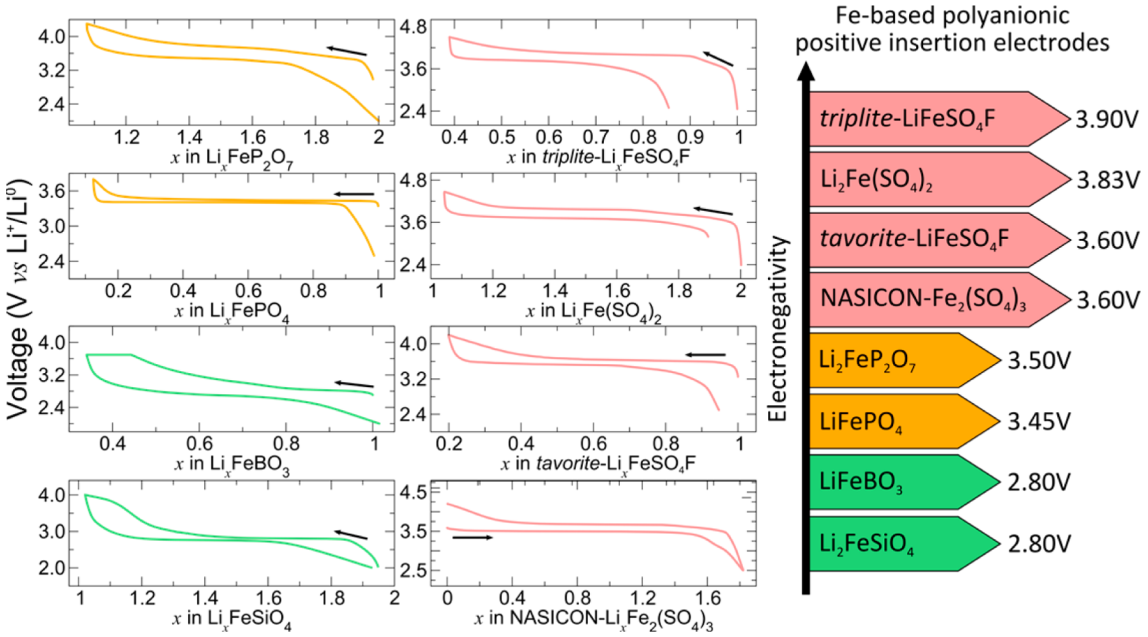

Figure 1. Electrochemical curves of several Fe-based polyanionic insertion electrodes. Representative charge−discharge cycles for several heavily studied Fe-based polyanionic materials. Note that the inductive effect, as originally proposed by J.B. Goodenough, explains changes in the potential with increasing electronegativity of the polyanionic group; however, as the SO_4 and PO_4 phases illustrate, it does not explain differences in the potential for the same polyanionic group. Data for Li_2FeSiO_4, $LiFeBO_3$, *olivine*-$LiFePO_4$, $LiFeP_2O_7$, *tavorite*-$LiFeSO_4F$, $Li_2Fe(SO_4)_2$, and *triplite*-$LiFeSO_4F$ were provided by the authors of refs 13−17, 11, and 10, respectively.

considerations, attempts to incorporate fluorine in oxide or polyanionic compounds were pursued to further enhance the ionic character of these bonds.[6−8] Indeed, our group recently demonstrated the ability to stabilize several new polymorphs of $LiFeSO_4F$, one of which is isostructural to the mineral *triplite* and operates at a potential of 3.90 V vs Li^+/Li^0; the highest potential for the Fe^{3+}/Fe^{2+} redox couple ever reported for an inorganic compound and at least 300 mV higher than most other Fe-SO_4-based materials.[9,10] Even though the exact origin of this very high potential was not immediately clear, it was not long before $Li_2Fe(SO_4)_2$ was discovered[11,12] and it too was found to operate at a comparably high potential of 3.83 V vs Li^+/Li^0.

Given the similar electrochemistry, it was not surprising that some features in the structures of *triplite* and $Li_2Fe(SO_4)_2$ were recognized to be topologically similar. In particular, the arrangement of SO_4 groups in the two compounds results in similar chains of Li/Fe octahedra, and therefore, comparable coordination environments for Fe as illustrated in panels a and b in Figure 2. This motivated a deeper investigation into trying to understand the source of these unusually high redox potentials, which we discuss in the following.

Before beginning, it is instructive to review the inductive effect as originally proposed by Goodenough.[4,5] At its simplest level, the inductive effect is a result of the electronegativity of the constituent elements in a compound altering the balance between the ionic and covalent character of the metal−ligand bonds. More electronegative elements draw more charge density toward their nuclei and thereby cause an increase in the ionic character of the bonds to the transition metal. As the ionicity of these bonds increases, the antibonding states associated with the Fe^{3+}/Fe^{2+} redox potential are pushed lower in energy and the open circuit voltage of the cell goes up. More fundamentally, however, it must be remembered that the ionocovalent character of the bonding in extended solids is

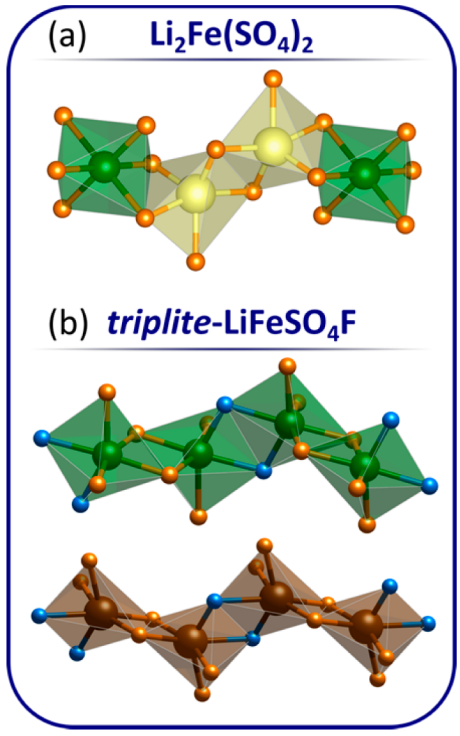

Figure 2. Comparison of the edge sharing chains of Fe and Li that exist in (a) $Li_2Fe(SO_4)_2$ and (b) the *triplite*-phase of $LiFeSO_4F$. Recall that the metal sites in *triplite* are randomly mixed. Iron sites are shown in green and brown, oxygen in orange, fluorine in blue, and lithium in light yellow.

determined from an amalgam of structural features which includes, but is not limited to: crystal field effects, regularity of the coordination environment, site energies, and unit cell volume. Thus, making an a priori prediction for how a material

dx.doi.org/10.1021/am405579h | ACS Appl. Mater. Interfaces 2014, 6, 10832−10839

may behave as an insertion electrode is an immensely challenging problem and new guidelines are desperately needed to increase the speed with which we can identify new and promising phases. Differences in electronegativity offer the simplest way to understand changes in the electrochemical performance when the structure of a material is held constant, as in NASICON or *tavorite*; however, it is highly nontrivial to understand the reasons for changes in the open circuit voltage across different compounds or polymorphs. For example, it may be tempting to attribute the increased potential in $Li_2Fe(SO_4)_2$ (3.83 V) when compared with *tavorite*-$LiFeSO_4F$ (3.60 V) to the increased number of charge-withdrawing SO_4 tetrahedra that are coordinated to each Fe octahedron (six instead of four); however, the redox centers in NASICON $Fe_2(SO_4)_3$ have a nearly identical coordination by six SO_4 groups yet only operate at 3.60 V. Hence, the number of polyanionic groups bound to each site alone does not appear to be a sufficient indicator for increased redox potentials. Additionally, if electronegativity really were the only relevant factor, $Li_2Fe(SO_4)_2$ would actually be expected to display a lower potential than all the polymorphs of $LiFeSO_4F$ because of the absence of fluorine; the most electronegative element in the periodic table. This, in fact, is clearly not the case and appears to be consistent with recent reports[18] claiming that the incorporation of fluorine does not guarantee an increased open circuit voltage. Thus, traditional arguments based purely around electronegativity are not always a sufficient predictor for the open circuit voltage.

A careful inspection of metal−ligand bond lengths can provide some insight into the character of the bonding since shorter bonds (which reflect an increase in orbital overlap) should intuitively be more covalent whereas longer bonds should be more ionic. This structural indicator can prove useful as a figure-of-merit as recently demonstrated in the polymorphs of Li_2FeSiO_4.[13] However, a metal−oxygen bond which is shared with a SO_4 group, as illustrated in Figure 3a, will always prove to be more ionic than a bond of the same length which is shared with a PO_4 group because of the difference in electronegativity, so comparisons between different polyanionic families often fails to be informative. It is also worth noting that accurate bond lengths cannot, under any circumstance, be determined from Rietveld refinements against powder diffraction data when a material is atomically disordered like the *triplite*-phase of $LiFeSO_4F$. The distance that is obtained from this type of analysis is actually an average value of the bond lengths for all the elements sharing the same site and cannot be trusted to reflect an accurate metal−ligand bond length.

Accordingly, considerable effort was dedicated to identifying a more appropriate structural descriptor which could be used to assist in the identification of new phases which may exhibit large redox potentials across a variety of polyanionic families. Upon inspection of several Fe-based insertion electrodes, which included SO_4-, SiO_4-, PO_4-, and P_2O_7-based phases, a common structural feature which was found to exhibit a strong correlation with trends in the redox potentials was the number of Li ions sitting in proximity to the transition metal. More specifically, the number of bonds that Fe and Li share to a common polyanionic group, as illustrated in Figure 3b, appears to track extremely well with the open circuit voltage. To illustrate this, the coordination environments of Fe in several polyanionic compounds were evaluated and are shown in Figures 4 and 5.

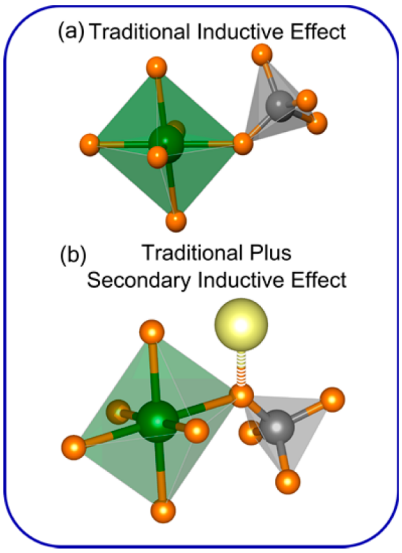

Figure 3. Illustration of the primary and secondary inductive effect. (a) Illustration of the bonding associated with the traditional primary inductive effect. (b) Illustration of the bonds associated with the secondary inductive as described in the text. The formation of this third interaction between lithium and oxygen is proposed to further increase the ionic character of the Fe−O bond, giving rise to larger potentials.

This is not the first time it has been suggested that the position of Li with respect to the redox center can influence the open circuit voltage of positive electrodes.[19−21] Indeed, the ability of alkaline metals to influence the ionocovalent character of transition-metal bonds has been demonstrated extensively by the work of Pouchard, Hagenmuller, et al.[22,23] Here, just as in the work of Pouchard, the rationale is straightforward. When Li occupies a site which is very close to the Fe−O polyhedra, there will be an interaction between the Li and O ions which are already bound to the Fe and SO_4 groups (see Figure 3b). The presence of this electropositive cation will pull additional charge density out of the existing Fe−O bond and further reduce its covalent character in addition to the effect that comes from the polyanionic group's electronegativity. This interaction with Li can also be viewed as the anions in the lattice becoming observably more overbonded and, as a result, unable to donate the same amount of charge density into the bonding interactions with the redox center.

It is important to note that because Li has one of the smallest electronegativities in the periodic table, its influence is certainly be expected to be small and it appears that multiple shared Li−O−Fe bonds are necessary in order to produce a cumulative effect which results in an observable change in the open circuit potential. Additionally, Li's influence only seems to play a role in situations where the metal−oxygen bonds have already been sufficiently weakened by the primary inductive effect from the polyanionic group. Thus, strongly covalent (shorter) bonds or bonds that are shared with an anion which is not part of a polyanionic group, such as the F in some of the fluorosulphates, are not as strongly influenced by interactions with Li. Hence, the influence of Li should be considered as a secondary inductive effect and should only be invoked when the primary inductive effect of Goodenough cannot fully explain the observed behavior. This implies that although Figures 4 and 5 display all the bonds between Fe and the surrounding ligands alongside the interaction with Li, only those bonds that also

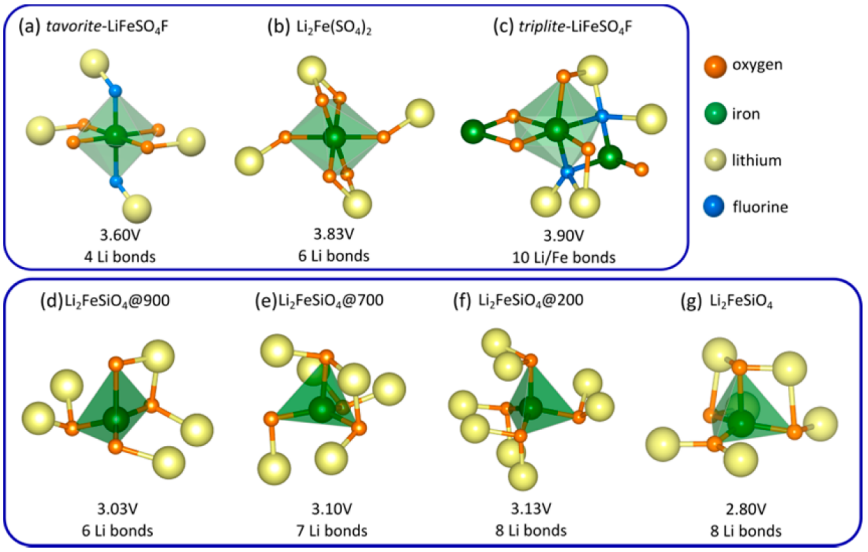

Figure 4. Illustration of the local environment of Fe and the metal–ligand bonds that are shared with Li in several (a–c) SO_4-based and (d–g) SiO_4-based compounds. Note that the increasing number of shared bonds with Li correlates well with the increase in potential across the series. The increasing number of Li neighbors can be considered as a reflection of the increasing ionic character of the bonds. It should also be recalled that the Fe–F bonds in the *tavorite* phase (a) and the Fe–O bonds in the Li_2FeSiO_4 phase (g) are significantly shorter than those in the other phases and therefore are not as likely to be affected by the presence of Li.

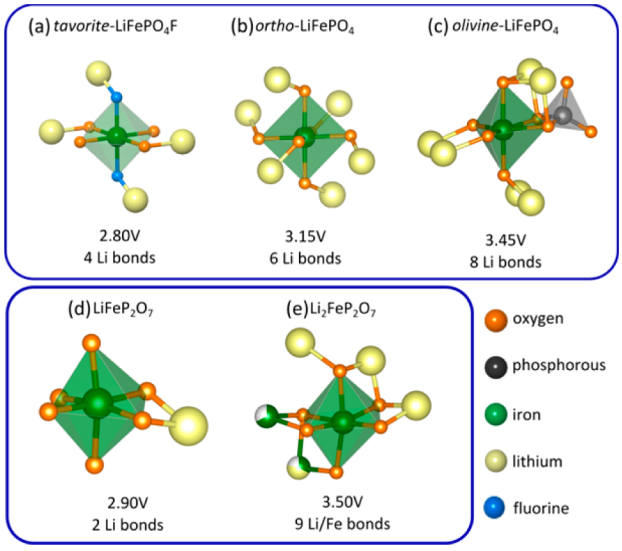

Figure 5. Illustration of the local environment of Fe and the metal–ligand bonds that are shared with Li in several (a–c) PO_4-based, and (d, e) P_2O_7-based compounds. Note that the increasing number of interactions with Li correlates well with the increase in potential across the series.

interact with Li in the manner discussed will experience this secondary effect and thereby result in a change in the potential.

To verify the robustness of this explanation, several polyanionic families were examined and their Fe coordination environment scrutinized. In the *tavorite* polymorph of $LiFeSO_4F$ (illustrated in Figure 4a), four Li ions sit near the FeO_4F_2 octahedra; however, the Fe–F distances are significantly shorter (~1.9 Å) than the Fe–O distances (~2.1 Å) and are not part of a polyanionic group. They will, therefore, not be expected to influence the bonding to the Fe. In the case of $Li_2Fe(SO_4)_2$, all six of the oxygen atoms in the octahedra interact with Li (Figure 4b), likewise all of the oxygen in *triplite* (Figure 4c) interact with a neighboring metal site. It should be noted, however, that due to the significant degree of site-mixing between the Fe and Li metals it is impossible to distinguish precisely how many bonds are shared with Li versus Fe and could vary anywhere from six in the fully site-ordered case to ten for an Fe that is completely surrounded by Li locally. Regardless, the number of interactions appears to always increase as the potential goes from 3.60 V in *tavorite* to 3.83 V in $Li_2Fe(SO_4)_2$ and finally 3.90 V in *triplite*.

Several polymorphs of Li_2FeSiO_4 also demonstrate an increasing number of Li–O–Fe interactions which is accompanied by an increase in potential from 3.03 to 3.16 V across the series[13] (see Figure 4d–f). It is interesting to note that for the most stable polymorph (see Figure 4g), which forms with extended exposure to air or upon full electrochemical oxidation, all of its Fe–O bonds interact with the surrounding Li, yet it exhibits only a 2.8 V potential. However, this is a similar situation to what was seen in *tavorite* as one can see upon closer inspection of the individual Fe–O bond lengths that this compound possesses significantly shorter, and therefore most covalent Fe–O bonds. So, as was already mentioned, it is unlikely that Li will influence the character of these bonds as strongly as in the other three phases.

Several phosphate-based phases were also examined, but the trivalent state of the PO_4 groups presents a challenge. The reader should recall that redox potentials are strongly influenced by the position of the antibonding states on Fe regardless of whether the starting compound contains Fe^{2+} or Fe^{3+}. That is to say, even though Li is inserted into $LiFePO_4F$ (Fe^{3+} reduced to Fe^{2+}) while it is removed from $LiFePO_4$ (Fe^{2+} oxidized to Fe^{3+}), the character of the bonds is still principally dictated by the structure at the beginning, rather than the structure at the end of cycling. Once this consideration is addressed, Figure 5a–c clearly shows that *olivine*-$LiFePO_4$ (3.45 V) is far more densely packed with Li than either $LiFePO_4F$ (2.80 V) or *ortho*-$LiFePO_4$ (3.15 V)[24] and the proposed rationale holds true. In fact, it is particularly interesting to mention that the FeO_6 octahedra in $LiFePO_4$ actually share an edge with the PO_4 groups, which is an unusual orientation for a

polyanionic group and may further help to explain the additional increase in the redox potential found in $LiFePO_4$. Finally, $LiFeP_2O_7$ and $Li_2FeP_2O_7$, which possess completely different structures in addition to the differences in their redox potentials, were also compared (see Figure 5d, e) and found to show the same correlation found in the other polyanionic families. Thus, structures containing Fe^{3+} appear to fit in with the trends seen for those containing Fe^{2+}; however, the proposed secondary inductive effect is clearly very weak compared with the primary effect of the polyanionic group so one must be careful not to overinterpret the influence of the Li-position without also taking into consideration the effects we have previously mentioned that can also affect the open circuit potential.

Indeed, although the structural features discussed up to this point clearly act as good qualitative indicators of experimental performance, it is obvious that a more rigorous way of describing and predicting the ionocovalent character of these materials would be extremely desirable; therefore, the remainder of the manuscript will focus on identifying a more quantitative indicator that can be used for the screening of new compounds. Considering their usefulness in approximating oxidation states and verifying structural models for crystallographers, bond valence sums (BVS)[25] would seem to offer a natural starting point in this pursuit. Unfortunately, this kind of analysis relies heavily on tabulated bonds lengths, which are the result of averaging bond lengths across several kinds of compounds in the literature. Thus, it is not surprising that we found no correlation between the BVS and the experimental voltages (see Table 1).

Table 1. Bond Valence Sums (BVS) on Fe and Experimental Open Circuit Voltage (OCV) for a Selection of Polyanionic Compounds

phase	BVS	OCV (V)
$Li_2Fe(SO_4)_2$	1.94	3.83
layered-$LiFeSO_4OH$	2.00	3.60
tavorite-$LiFeSO_4F$	2.05	3.60
olivine-$LiFePO_4$	1.90	3.45
ortho-$LiFePO_4$	2.07	3.15
Li_2FeSiO_4-900	1.90	3.03
Li_2FeSiO_4-700	1.81	3.10
Li_2FeSiO_4-200	1.55	3.13
Li_2FeSiO_4	2.26	2.80
$LiFeBO_3$	1.98	2.80

A natural progression from BVS analysis is to employ more system-independent computational tools to provide a time-efficient and less empirical method for determining the nature of bonding in these materials. As such, we analyzed several structures containing a variety of polyanionic groups using the partial atomic charge and hardness analysis (PACHA) formalism,[26] which is described in detail in the Methods section. We applied this analysis to several compounds which were chosen for the reliability of the structural data, availability of electrochemical data, and absence of atomic disorder. The results from the PACHA analysis, shown in panels a and b in Figure 6, demonstrate that the experimental open circuit voltage increases as the mean electronegativity increases, giving a sound theoretical explanation to the observed redox potentials. It is worth noticing that the *ortho*-$LiFePO_4$ (red diamond at 3.15 V)[24] is actually found to have a higher mean

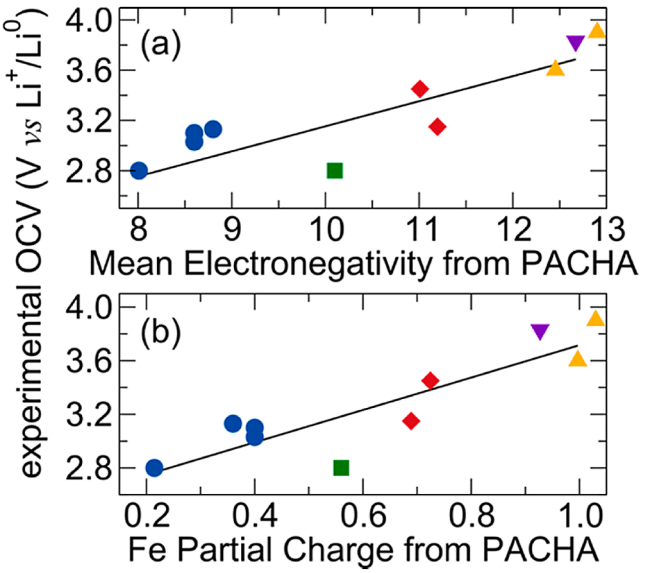

Figure 6. Correlation between computed parameters from PACHA and OCV. Dependence of the experimental open circuit voltage OCV on the (a) mean electronegativity and (b) Fe partial charge from the PACHA analysis phases with the general composition $LiFePO_4$ are marked with a red diamonds, the polymorphs of Li_2FeSiO_4 are marked with blue circles, $LiFeBO_3$ is with a green square, *tavorite* and *triplite*-$LiFeSO_4F$ are marked with orange triangles pointing upward, and $Li_2Fe(SO_4)_2$ is marked with a purple triangle pointing downward.

electronegativity than the more heavily studied *olivine*-$LiFePO_4$ (red diamond at 3.45 V). In this case, it is possible to attribute the difference in open circuit voltage between the two polymorphs to the large iron partial charge that is found in the orthorhombic polymorph as compared to the one in the *olivine* one (Figure 6b). Two main reasons may be invoked to explain these difficulties. First, in PACHA the Madelung potential is evaluated using a Ewald summation in order to ensure a full convergence of the partial charge distributions. Consequently, small errors in the lithium position may have large effects on the mean electronegativity. Partial charges, on the other hand, are much less sensitive to these long-range Madelung effects. It is worth noticing that in the orthorhombic polymorph, the lithium is coordinated by just four oxygen atoms but moving just slightly could lead to a 6-fold coordination as in the *olivine* polymorph. Second, the spherical charge approximation in PACHA requires a linear variation of electronegativity with the partial charge. This is not possible with alkaline elements owing to steep discontinuities which exist in ionization potentials after removal of the only valence electron. This approximation thus seems to be justified for structures that do not display the same stoichiometry, but fails for true polymorphs that only differ by the spatial arrangement of the atoms.

Hence, it appears that ab initio calculations based on density functional theory (DFT), which can fully characterize all of the quantum mechanical behavior of these systems are absolutely necessary to accurately describe changes in the bonding of these systems. DFT also opens the possibility of studying systems with less-well-defined experimental structures where the position of very light elements like protons on hydroxyl groups or Li are difficult to determine experimentally. Bader analysis, which partitions the calculated charge density into discrete atoms using a well-defined mathematical criterion,

allows one to determine the total electronic charge residing on each atom and thereby quantify the ionocovalent character of the bonding. Within this scheme (see the methods section for a more detailed description), larger values reflect a more ionic character with smaller values indicating more covalency. Thus, the application of Bader analysis to determine the character of bonds has recently proven to be particularly powerful for a range of solid state compounds.[27,28]

As shown in Figure 7, regardless of the polyanionic group, there is clear evidence for an increasing ionic character on the Fe in each compound that correlates well with increases in the experimental open circuit potential. The Bader charge of the other elements in the composition can be found in Table 2. An interesting result is that for all of the structures we have done calculation on, the Bader charge associated with Li appears to be roughly constant around +0.86.

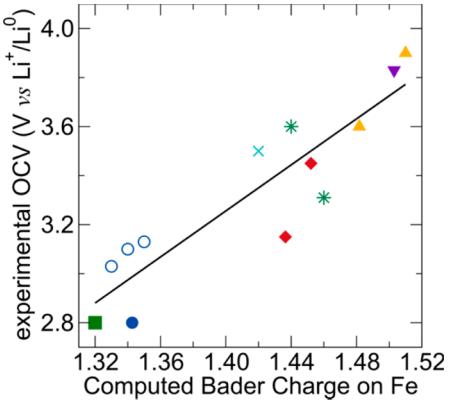

Figure 7. Correlation between the Bader charge and OCV. Correlation between the Bader charge on Fe as calculated using density functional theory calculations and the experimental open circuit voltage. Phases with the general composition $LiFePO_4$ are marked with red diamonds, the polymorphs of Li_2FeSiO_4 with blue circles, $LiFeBO_3$ with a green square, *tavorite* and *triplite*-$LiFeSO_4F$ with orange triangles pointing upward, $Li_2Fe(SO_4)_2$ with a purple triangle pointing downward, $LiFeSO_4OH$ with green asterisks, and Li_2FePO_4F is marked with a cyan cross. Note that the unfilled symbols, cross, and asterisks correspond to the structures that are not well understood experimentally and were optimized using structural relaxations. The data point for Li_2FePO_4F was taken from ref 42.

Lastly, we note that in terms of classical thermodynamic arguments, the open circuit voltage of a battery is usually taken as the difference in the total free energy of the delithiated and lithiated forms of the cathode. From this perspective, the creation of more ionic interactions that must be broken and reformed on reversible insertion of Li should clearly result in an increased open circuit voltage. This is consistent with our finding which once again does not require knowledge of the structure in the delithiated phase to rank materials with respect to each other in terms of redox potentials.

In summary, we have presented several structural and computational indicators which can be used to identify new Fe-based electrodes with exceptionally large potentials. In the course of this discussion, we have identified what looks to be a secondary inductive effect in polyanionic materials that results from the reallocation of charge density as Li is inserted into a structure. This effect is easily explained using the PACHA formalism within the framework of the spherical charge approximation of DFT equations. This formalism shows that any increase in open circuit voltage should be linked to an increase in Fe partial charge (iono-covalency effects) and/or an increase in the Madelung potential (inductive effects) experienced at the iron site. More interestingly, we have demonstrated through the use of two very different computational approaches that the experimental voltages of these materials correspond well with calculated values such as the Bader charge and the PACHA electronic chemical potential of Fe within the structure. More simply, the ideas presented here can be considered to reflect the general trend that more densely packed compounds tend to have a higher ionic character to their bonds and therefore demonstrate higher redox potentials. This observation implies a delicate balance in the design of new Fe-based materials between the desire for an open framework structure which allows facile diffusion of ions and densely packed structures to give the largest potentials possible at the risk of exhibiting poor electrode kinetics. We also wish to point out that although it has been well-demonstrated that the open circuit voltage of materials can be readily approximated using ab initio calculations, an accurate understanding of the delithiated structure is critical in order for these values to be reliable. If the delithiated structure is unknown, and structural relaxations fail to accurately predict it, the calculated redox potential will not be accurate and ab initio approaches may miss a truly promising

Table 2. Complete List of the Bader Charge Associated with Each Element in the Selected Compounds[a]

	Li	Fe	P	S	Si	B	F	O	H	OCV(V)
triplite-$LiFeSO_4F$	+0.88	+1.51		+3.93			−0.79	−1.38		3.90
$Li_2Fe(SO_4)_2$	+0.87	+1.50		+3.94				−1.38		3.83
tavorite-$LiFeSO_4F$	+0.87	+1.48		+3.89			−0.76	−1.37		3.60
layered-$LiFeSO_4OH$	+0.87	+1.44		+3.90				−1.36	+0.61	3.60
Li_2FePO_4F	+0.86	+1.42	+3.62				−0.81	−1.50		3.50
olivine-$LiFePO_4$	+0.87	+1.45	+3.68					−1.50		3.45
tavorite-$LiFeSO_4OH$	+0.87	+1.46		+3.92				−1.37	+0.61	3.31
ortho-$LiFePO_4$	+0.87	+1.44	+3.69					−1.50		3.15
Li_2FeSiO_4 @200	+0.85	+1.35			+3.08			−1.53		3.13
Li_2FeSiO_4 @700	+0.85	+1.34			+3.13			−1.54		3.10
Li_2FeSiO_4 @900	+0.85	+1.33			+3.12			−1.54		3.03
Li_2FeSiO_4	+0.85	+1.34			+3.13			−1.54		2.80
$LiFeBO_3$	+0.85	+1.32				+2.34		−1.50		2.80

[a]OCV is the experimental open circuit voltage and the Li_2FeSiO_4 polymorphs are labeled according to the notation of Masquelier et al. in ref 13. Note that the data on Li_2FePO_4F were reproduced from ref 42.

phase. Thus, most importantly, the structural features and Bader charge as described above should serve as valuable new figures-of-merit for the prediction and identification of new and higher-performing Fe-based cathode materials in these high-throughput computational searches. Yet, in order for the charge on Fe to act as a true indicator, it is clear that the community of computational chemists and physicists need to develop more robust and accurate ways to quantify the covalent versus ionic character of these compounds.

METHODS

Partial Atomic Charge and Hardness Analysis (PACHA). This approach is based on a powerful density functional theory (DFT) theorem identifying electronegativity as a measure of the negative of the electronic chemical potential.[30] Both redox potential and electronegativity are a measure of the affinity of a substance for electrons as shown in the series: Li (−3.05 V, 1.0), Al (−1.66 V, 1.5), Fe (−0.44 V, 1.8), I (+0.54 V, 2.5), Cl (+1.36 V, 3.0), and F (+2.87 V, 4.0) where the second number is the well-known Pauling electronegativity. Consequently, the higher the electronegativity becomes, the lower the electronic chemical potential (i.e., the HOMO energy for a molecule or the Fermi level for a solid) and hence the more positive the redox potential becomes. The PACHA formalism has the advantage of implementing the rigorous DFT-based electronegativity equalization principle using a nonempirical atomic parametrization based on the use of Allen's electronegativity scale[29,31] and on the radius R_i of the most diffuse valence orbital derived by relativistic quantum-mechanical methods for approximating chemical hardness.[32] Using a spherical charge approximation of DFT equations, it is possible to express the electronegativity of an atom EN in any substance as a sum of three terms: the Allen's electronegativity χ_i(V), the product of its chemical hardness $[\eta_i(\mathrm{V}) = \mathrm{e}/(4\pi\varepsilon_0 R_i)]$ by its partial charge q_i and the Madelung potential times the partial charge $[\varphi_i(\mathrm{V}) = (\mathrm{e}/(4\pi\varepsilon_0))(\Sigma_j q_j/R_{ij})]$: $\mathrm{EN} = \chi_i + \eta_i q_i + \varphi_i q_i$. As all three terms are in volts and as EN should be the same for all atoms, it is possible to anticipate a direct correlation between EN and the redox potential. This expression shows that the redox potential may be increased either by increasing atomic electronegativity of the redox center χ_i, increasing the positive partial charge q_i (i.e., by surrounding the redox center with electronegative elements), contracting atomic orbitals of the redox center (decrease in R_i), or increasing the Madelung potential, i.e., bringing large positive charges q_j close to the redox center (small R_{ij}). The first three factors (χ_i, η_i, q_i) explain why the higher the ionicity, the higher the redox potential, whereas the Madelung term explains why the higher the number of Li interactions, the higher the redox potential.

Density Functional Theory Calculations. The structure and total energy of the bulk compounds ($LiFeBO_3$, *ortho*-$LiFePO_4$, *triplite*- and *tavorite*-$LiFeSO_4F$, $Li_2Fe(SO_4)_2$, as well as the polymorphs of Li_2FeSiO_4 and $LiFeSO_4OH$) were obtained using a plane-wave DFT method, as implemented in the code VASP.[33,34] The Perdew-Burke-Ernzerhof gradient corrected functional, revised specifically for solids (PBEsol)[35] was used to treat the exchange and correlation, with $+U$ correction of 4 eV applied to the Fe d states.[36] The frozen-core electrons were treated within the projector augmented-wave method.[37,38] Structural optimizations of each compound were performed at a series of volumes in order to calculate the equilibrium lattice parameters. In each case the atomic positions, lattice vectors and cell angles were allowed to relax, whereas the total volume was held constant. The resulting energy volume curves were fitted to the Murnaghan[39] equation of state to obtain the equilibrium bulk cell volume. This approach avoids the problems of Pulay stress and changes in basis set which can accompany volume changes in plane wave calculations. For the tavorite-$LiFeSO_4OH$, which did not have a defined crystal structure available, we tested many positions of Li within the $FeSO_4OH$ cell, allowing the cell and all atomic positions to relax, with the results of the lowest energy structure used to calculate the Bader charges presented. A plane-wave cutoff of 750 eV was used to define the basis set, with well-converged k-point sampling for each of the compounds [e.g., $8 \times 6 \times 6$ Γ-point centered mesh was used for $Li_2Fe(SO_4)_2$]. All calculations were spin polarized to account for the antiferromagnetic ordering in these materials. Structural optimizations were considered converged when the force on every ion was less than 0.01 eV $Å^{-1}$. To quantify the distribution of charges in these systems, we have performed Bader analysis[40] using the program developed by the Henkelman group.[41]

To analyze the Bader charge on the atomically disordered *triplite* phase of $LiFeSO_4F$, four separate low-energy atomic configurations as determined in the work of Yamada et al. were calculated and analyzed. All results yielded essentially the same Bader charge of $+1.51e$ on each Fe and therefore this value was taken as representative.

Bader Analysis. Quantum chemical theory does not directly define atomic charges in molecules or solids. DFT outputs the electron density, which in the framework of a plane wave basis set scheme, makes determining how the electrons should be partitioned quite difficult. In quantum chemistry, the most commonly used partioning scheme is the Mulliken analysis, but this approach is predicated on localized basis sets, and therefore in not appropriate for our DFT systems. Instead we use the Bader[40] charge analysis method (Atoms in Molecules, AIM), using the program developed by Henkelman et al.[41] In this scheme, we define an atomic volume as that region of space, including the nucleus, which lies within all zero flux surfaces surrounding the nucleus. We start at a maximum in the electron density (at the nucleus) and work outward (opposite direction to density gradient) until the gradient reaches zero and starts to rise again. At the zero point, we have a bond between two atoms. In AIM theory, the partial atomic charge is the difference between the nuclear charge and the number of electrons residing within an atomic basin (number of electrons is the integral of the density over space)

$$\mathrm{k}q_k = Z_k - \int_{\Omega_k} \rho(r)dr$$

where the volume of the atomic basin (the zero flux surface) is given by Ω_k.

AUTHOR INFORMATION

Corresponding Author

*E-mail: jean-marie.tarason@college-de-france.fr.

Notes

The authors declare no competing financial interest.

ACKNOWLEDGMENTS

The authors acknowledge John B. Goodenough, Ken R. Poeppelmeier, and J. M. Rondinelli for their careful reading of the manuscript and valuable feedback. N. Recham and M. Ati are thanked for helpful discussions. The authors are also grateful to P. Barpanda for providing the structural information on the *triplite* phase of $LiFeSO_4F$ that was used for the Bader analysis. J.M.T. thanks G. Ferey for looking at the valence approach and suggesting the use of PACHA formalism. D.O.S. is grateful to the Ramsay Memorial Trust and University College London for the provision of a Ramsay Fellowship. All UCL calculations were made possible by the UKs HPC Materials Chemistry Consortium, which is funded by the EPSRC (Grant EP/F067496). M.R. acknowledges the French "Ministère de l'Enseignement Supérieur et de la Recherche" for her Ph.D. Grant. B.C.M. acknowledges start-up funding support from the Dana and David Dornsife College of Letters and Sciences at the University of Southern California.

REFERENCES

(1) Nagaura, T.; Tozawa, K. Lithium Ion Rechargeable Battery. *Prog. Batteries Solar Cells* **1990**, *9*, 209.

(2) Tarascon, J.-M.; Armand, M. Issues and Challenges Facing Rechargeable Lithium Batteries. *Nature* **2001**, *414*, 359−367.
(3) Armand, M.; Tarascon, J.-M. Building Better Batteries. *Nature* **2008**, *451*, 652−657.
(4) Padhi, A. K.; Nanjundaswamy, K. S.; Masquelier, C.; Goodenough, J. B. Mapping of Transition Metal Redox Energies in Phosphates with NASICON Structure by Lithium Intercalation. *J. Electrochem. Soc.* **1997**, *144*, 2581−2586.
(5) Padhi, A. K.; Manivannan, V.; Goodenough, J. B. Tuning the Position of the Redox Couples in Materials with NASICON Structure by Anionic Substitution. *J. Electrochem. Soc.* **1998**, *145*, 1518−1520.
(6) Barker, J.; Saidi, M. Y.; Swoyer, J. L. Lithium Metal Fluorophosphate Materials and Preparation Thereof. Patent WO 2001/084655, November 8, 2001.
(7) Saidi, M. Y.; Barker, J.; Huang, H.; Swoyer, J. L.; Adamson, G. Electrochemical Properties of Lithium Vanadium Phosphate as a Cathode Material for Lithium-Ion Batteries. *Electrochem. Solid-State Lett.* **2002**, *5*, A149−A151.
(8) Barker, J.; Saidi, M. Y.; Swoyer, J. L. Electrochemical Insertion Properties of the Novel Lithium Vanadium Fluorophosphate, $LiVPO_4F$. *J. Electrochem. Soc.* **2003**, *150*, A1394−A1398.
(9) Barpanda, P.; Ati, M.; Melot, B. C.; Rousse, G.; Chotard, J.-N.; Doublet, M.-L.; Sougrati, M. T.; Corr, S. A.; Jumas, J.-C.; Tarascon, J.-M. A 3.90 V Iron-Based Fluorosulphate Material for Lithium-Ion Batteries Crystallizing in the Triplite Structure. *Nat. Mater.* **2011**, *10*, 772−779.
(10) Ati, M.; Melot, B. C.; Chotard, J.-N.; Rousse, G.; Reynaud, M.; Tarascon, J.-M. Synthesis and Electrochemical Properties of Pure $LiFeSO_4F$ in the Triplite Structure. *Electrochem. Commun.* **2011**, *13*, 1280−1283.
(11) Reynaud, M.; Ati, M.; Melot, B. C.; Sougrati, M. T.; Rousse, G.; Chotard, J.-N.; Tarascon, J.-M. $Li_2Fe(SO_4)_2$ as a 3.83V Positive Electrode Material. *Electrochem. Commun.* **2012**, *21*, 77−80.
(12) Reynaud, M.; Ati, M.; Chotard, J.-N.; Tarascon, J.-M. Sulfates Utiles Comme Matériaux D'électrode. Patent FR 12 51854, filed February 29, 2012.
(13) Sirisopanaporn, C.; Masquelier, C.; Bruce, P. G.; Armstrong, A. R.; Dominko, R. Dependence of Li_2FeSiO_4 Electrochemistry on Structure. *J. Am. Chem. Soc.* **2010**, *133*, 1263−1265.
(14) Tao, L.; Rousse, G.; Chotard, J. N.; Dupont, L.; Bruyère, S.; Hanžel, D.; Mali, G.; Dominko, R.; Levasseur, S.; Masquelier, C. Preparation, Structure and Electrochemistry of $LiFeBO_3$: A Cathode Material for Li-Ion Batteries. *J. Mater. Chem. A* **2014**, *2*, 2060−2070.
(15) Recham, N.; Dupont, L.; Courty, M.; Djellab, K.; Larcher, D.; Armand, M.; Tarascon, J.-M. Ionothermal Synthesis of Tailor-Made $LiFePO_4$ Powders for Li-Ion Battery Applications. *Chem. Mater.* **2009**, *21*, 1096−1107.
(16) Nishimura, S.; Nakamura, M.; Natsui, R.; Yamada, A. New Lithium Iron Pyrophosphate as 3.5 V Class Cathode Material for Lithium Ion Battery. *J. Am. Chem. Soc.* **2010**, *132*, 13596−13597.
(17) Recham, N.; Chotard, J.-N.; Dupont, L.; Delacourt, C.; Walker, W.; Armand, M.; Tarascon, J.-M. A 3.6 V Lithium-Based Fluorosulphate Insertion Positive Electrode for Lithium-Ion Batteries. *Nat. Mater.* **2010**, *9*, 68−74.
(18) Armand, M.; Tarascon, J.-M.; Arroyo-de Dompablo, M. E. Comparative Computational Investigation of N and F Substituted Polyoxoanionic Compounds: The Case of Li_2FeSiO_4 Electrode Material. *Electrochem. Commun.* **2011**, *13*, 1047−1050.
(19) Goodenough, J. B.; Kim, Y. Challenges for Rechargeable Li Batteries. *Chem. Mater.* **2013**, *22*, 587−603.
(20) Gutierrez, A.; Benedek., N. A. Crystal-Chemical Guide for Understanding Redox Energy Variations of $M^{2+/3+}$ Couples in Polyanion Cathodes for Lithium-Ion Batteries. *Chem. Mater.* **2013**, *25*, 4010−4016.
(21) Goodenough, J. B. *Design Considerations* **1994**, *69*, 184−198.
(22) Hayashi, K.; Demazeau, G.; Pouchard, M.; Hagenmuller, P. Preparation and Magnetic Study of a New Iridium (V) Perovskite: $LaLi_{0.5}Ir_{0.5}O_3$. *Mater. Res. Bull.* **1980**, *15*, 461−467.
(23) Demazeau, G.; Zhu, L.-M.; Fournes, L.; Pouchard, M.; Hagenmuller, P. Two New iron(IV) Oxides with High-Spin Configuration: $SrLaMg_{0.50}Fe_{0.50}O_4$ and $SrLaZn_{0.50}Fe_{0.50}O_4$. *J. Solid State Chem.* **1988**, *72*, 31−37.
(24) Voß, B.; Nordmann, J.; Kockmann, A.; Piezonka, J.; Haase, M.; Taffa, D. H.; Walder, L. Facile Synthesis of the High-Pressure Polymorph of Nanocrystalline $LiFePO_4$ at Ambient Pressure and Low Temperature. *Chem. Mater.* **2012**, *24*, 633−635.
(25) Brown, I. D.; Altermatt, D. Bond-Valence Parameters Obtained from a Systematic Analysis of the Inorganic Crystal Structure Database. *Acta Crystallogr. B* **1985**, *41*, 244−247.
(26) Henry, M. Nonempirical Quantification of Molecular Interactions in Supramolecular Assemblies. *ChemPhysChem* **2002**, *3*, 561−569.
(27) Kurzman, J. A.; Moffitt, S. L.; Llobet, A.; Seshadri, R. Neutron Diffraction Study of La_4LiAuO_8: Understanding Au^{3+} in an Oxide Environment. *J. Solid State Chem.* **2011**, *184*, 1439−1444.
(28) Scanlon, D. O.; Godinho, K. G.; Morgan, B. J.; Watson, G. W. Understanding Conductivity Anomalies in CuI-Based Delafossite Transparent Conducting Oxides: Theoretical Insights. *J. Chem. Phys.* **2010**, *132*, 024707−024717.
(29) Mann, J. B.; Meek, T. L.; Allen, L. C. Configuration Energies of the Main Group Elements. *J. Am. Chem. Soc.* **2000**, *122*, 2780−2783.
(30) Parr, R. G.; Donnelly, R. A.; Levy, M.; Palke, W. E. Electronegativity: The Density Functional Viewpoint. *J. Chem. Phys.* **1978**, *68*, 3801−3807.
(31) Mann, J. B.; Meek, T. L.; Knight, E. T.; Capitani, J. F.; Allen, L. C. Configuration Energies of the D-Block Elements. *J. Am. Chem. Soc.* **2000**, *122*, 5132−5137.
(32) Waber, J. T.; Cromer, D. T. Orbital Radii of Atoms and Ions. *J. Chem. Phys.* **1965**, *42*, 4116−4123.
(33) Kresse, G.; Hafner, J. Ab Initio Molecular-Dynamics Simulation of the Liquid-Metal−amorphous-Semiconductor Transition in Germanium. *Phys. Rev. B* **1994**, *49*, 14251−14269.
(34) Kresse, G.; Furthmüller, J. Efficiency of Ab-Initio Total Energy Calculations for Metals and Semiconductors Using a Plane-Wave Basis Set. *Comput. Mater. Sci.* **1996**, *6*, 15−50.
(35) Perdew, J. P.; Ruzsinszky, A.; Csonka, G. I.; Vydrov, O. A.; Scuseria, G. E.; Constantin, L. A.; Zhou, X.; Burke, K. Restoring the Density-Gradient Expansion for Exchange in Solids and Surfaces. *Phys. Rev. Lett.* **2008**, *100*, 136406.
(36) Ramzan, M.; Lebègue, S.; Ahuja, R. Ab Initio Study of Lithium and Sodium Iron Fluorophosphate Cathodes for Rechargeable Batteries. *Appl. Phys. Lett.* **2009**, *94*, 151904.
(37) Blöchl, P. E. Projector Augmented-Wave Method. *Phys. Rev. B* **1994**, *50*, 17953−17979.
(38) Kresse, G.; Joubert, D. From Ultrasoft Pseudopotentials to the Projector Augmented-Wave Method. *Phys. Rev. B* **1999**, *59*, 1758−1775.
(39) Murnaghan, F. D. The Compressibility of Media under Extreme Pressures. *Proc. Natl. Acad. Sci. U.S.A.* **1944**, *30*, 244−247.
(40) Bader, R. F. W. *Atoms in Molecules−A Quantum Theory*; Oxford University Press: Oxford, U.K., 1990.
(41) Tang, W.; Sanville, E.; Henkelman, G. A Grid-Based Bader Analysis Algorithm without Lattice Bias. *J. Phys.: Condens. Matter* **2009**, *21*, 084204.
(42) Ramzan, M.; Lebegue, S.; Larsson, P.; Ahuja, R. Structural, Magnetic, And Energetic Properties of Na_2FePO_4F, Li_2FePO_4F, $NaFePO_4F$, and $LiFePO_4F$ from Ab Initio Calculations. *J. Appl. Phys.* **2009**, *106*, 043510.